Two-dimensional 2γ angular correlation study of delocalized positronium in alkali halides

1997 J. Phys.: Condens. Matter 9 11239

(http://iopscience.iop.org/0953-8984/9/50/024)

J. Phys.: Condens. Matter **9** (1997) 11239–11246. Printed in the UK PII: S0953-8984(97)86915-9

Two-dimensional 2γ angular correlation study of delocalized positronium in alkali halides

Yasuyoshi Nagai†, Haruo Saito†, Yasuyuki Nagashima†, Nobuhiko Kobayashi‡ and Toshio Hyodo†

† Institute of Physics, Graduate School of Arts and Sciences, University of Tokyo, 3-8-1 Komaba, Meguro-ku, Tokyo 153, Japan

‡ Department of Physics, Graduate School of Science, University of Tokyo, 7-3-1 Hongo, Bunkyo-ku, Tokyo 113, Japan

Received 13 August 1997, in final form 20 October 1997

Abstract. The two-dimensional angular correlation of positron annihilation radiation (2D-ACAR) from KCl and KI single crystals at low temperatures has been measured. The intensities of the narrow peaks resulting from the Bloch modulation of the delocalized positronium (Ps) are studied. The intensities of the peaks except for those at the momenta corresponding to the (000) and (200) reciprocal-lattice vectors are very low for both KCl and KI. The experimental results for KCl are compared with the calculations made by Zhang and Song. Calculations with simpler approximations are also performed for both KCl and KI.

1. Introduction

Positronium (Ps), the bound state of an electron and a positron, is unique in that information about its wave function $\phi(\boldsymbol{r}_e, \boldsymbol{r}_p)$, where $\boldsymbol{r}_e$ and $\boldsymbol{r}_p$ are the coordinates of the electron and the positron, respectively, is directly provided by the measurements of the one-dimensional (1D-) or two-dimensional (2D-) angular correlation of annihilation radiation (ACAR) [1]. The 1D- and 2D-ACAR are proportional to the linear and planar projections of the translational momentum density distribution

$$R(\boldsymbol{p}) \propto \left| \sum_i n_i \int \phi_i(\boldsymbol{r}, \boldsymbol{r}) \mathrm{e}^{-\mathrm{i}\boldsymbol{p}\cdot\boldsymbol{r}/\hbar} \, \mathrm{d}^3\boldsymbol{r} \right|^2 \tag{1}$$

of the annihilating electron–positron pair, respectively. Here, n_i is the occupation probability of the Ps state $\phi_i(\boldsymbol{r}_e, \boldsymbol{r}_p)$.

Ps forms in many insulating solids [2–4]. The Ps is in the delocalized Bloch state in quartz, ice, magnesium fluoride, and some alkali halides [5–8]. The delocalized Ps in alkali halides is observed only at low temperatures; it is self-trapped above some temperature characteristic of each material.

The wave function $\phi_{\boldsymbol{k}}(\boldsymbol{r}_e, \boldsymbol{r}_p)$ of delocalized Ps travelling with a translational wave vector $\boldsymbol{k}$ has the symmetry of the crystal, and the electron–positron overlap amplitude $\phi_{\boldsymbol{k}}(\boldsymbol{r}, \boldsymbol{r})$ can be expanded in terms of the reciprocal-lattice vector $\boldsymbol{G}$ as

$$\phi_{\boldsymbol{k}}(\boldsymbol{r}, \boldsymbol{r}) \propto \sum_{\boldsymbol{G}} u_{\boldsymbol{G}}(\boldsymbol{k}) \mathrm{e}^{\mathrm{i}(\boldsymbol{k}+\boldsymbol{G})\cdot\boldsymbol{r}}. \tag{2}$$

0953-8984/97/5011239+08$19.50

The occupation probability for the delocalized Ps thermalized at the bottom of its energy band can be approximated as $n_{\boldsymbol{k}} = \delta_{\boldsymbol{k},0}$. The momentum density distribution $R(\boldsymbol{p})$ for this state is

$$R(\boldsymbol{p}) \propto \sum_{\boldsymbol{k}} \sum_{\boldsymbol{G}} \delta_{\boldsymbol{k},0} |u_{\boldsymbol{G}}(\boldsymbol{k})|^2 \delta_{\boldsymbol{k},\boldsymbol{p}/\hbar-\boldsymbol{G}} = \sum_{\boldsymbol{G}} |u_{\boldsymbol{G}}(0)|^2 \delta_{\boldsymbol{p},\hbar\boldsymbol{G}}. \tag{3}$$

Accordingly the ACAR for the delocalized Ps has a sharp central and satellite peaks at the projections of the momenta corresponding to the reciprocal-lattice vectors.

Kasai and Fujiwara [9] have reported the ratio of the peak at the momentum corresponding to the (200) reciprocal-lattice vector to that of the central peak for KI measured by the 1D-ACAR method. They have also reported that the peaks corresponding to the odd Miller indices are not detectable even for KI and NaI. This is in contrast to the case of x-ray diffraction, where the odd-index reflections are very weak only for those alkali halides where the anion and the cation electron configurations are the same [10].

Recently, the relative intensities of the central and some satellite peaks for NaF, NaCl, and KCl were calculated by Zhang and Song [11, 12] using the extended-ion method to account for this interesting effect. Their calculations show that the odd-index satellite peaks are practically reduced to zero. A quantitative comparison between their results and the experimental values, however, has not been made because of the lack of corresponding experimental data; the intensity of the 1D projection of the (200) peak for KI, which is the only case for which an experimental value is available [9], is not included in their calculation.

In the present work, we measure the intensities of the Ps peaks for KCl single crystal at low temperature using the 2D-ACAR method in order to compare with the calculation made by Zhang and Song. A similar measurement for KI is also performed. The 2D-ACAR measurement is more sensitive to the fine structure of the momentum distribution than the 1D-ACAR measurement because the former integrates the momentum distribution along only one direction:

$$N_{2D}(p_x, p_y) = \int R(\boldsymbol{p})\ \mathrm{d}p_z \tag{4}$$

while the latter integrates it along two directions:

$$N_{1D}(p_x) = \iint R(\boldsymbol{p})\ \mathrm{d}p_y\ \mathrm{d}p_z. \tag{5}$$

We have observed very low but finite intensities of the odd-index peaks in KI which were not observed before. We also report that the intensities of the even-index peaks other than (200) are very low for both KCl and KI crystals, which constitutes another contrast to the case of x-ray diffraction. Two simple calculations of the wave functions of the Bloch-state Ps are performed to allow us to discuss such characteristics of the Ps peaks.

2. Experiments

The measurements were performed with newly developed 2D-ACAR apparatus using BGO scintillator arrays coupled to position-sensitive photomultiplier tubes [13]. The distance from the sample to the detectors is 5 m. One detector scans horizontally while the other scans vertically. The overall momentum resolution was $(1.1 \times 10^{-3}\,mc) \times (1.1 \times 10^{-3}\,mc)$ (m: free-electron mass; c: speed of light; $mc = 137$ au), which is moderate but good enough for measuring the intensities of the Ps peaks.

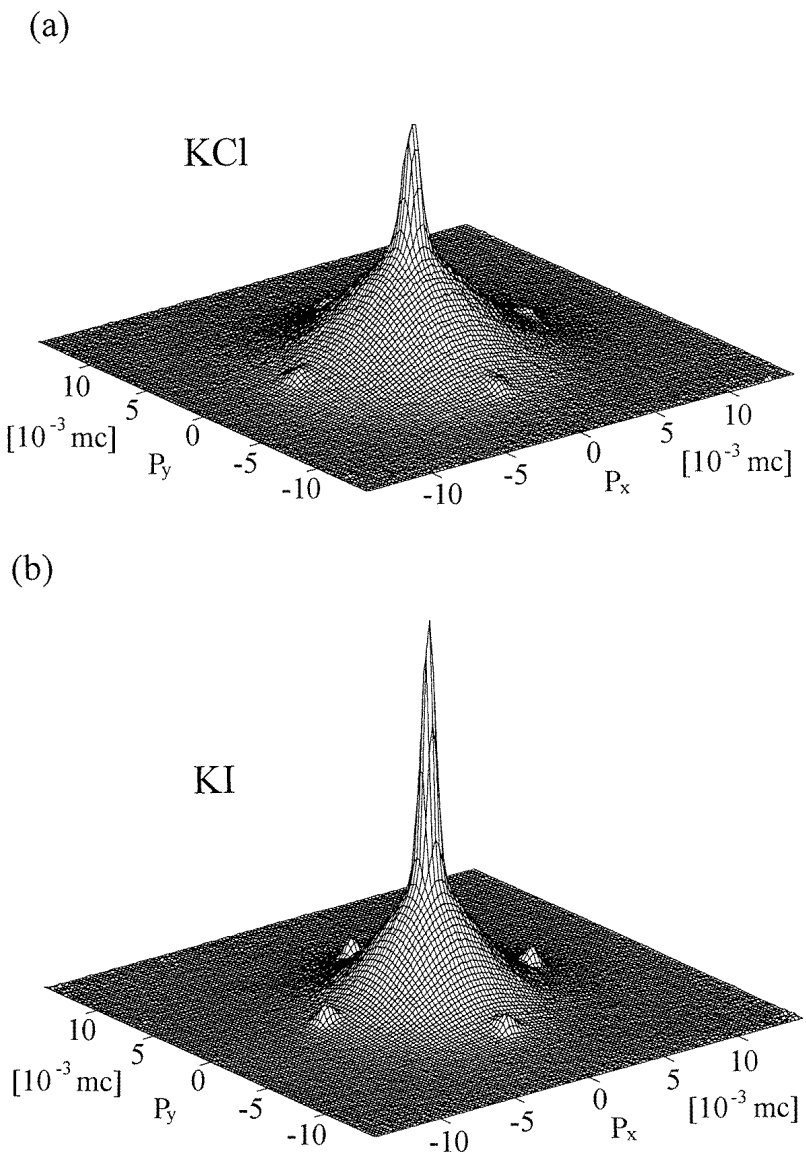

Figure 1. 2D-ACAR spectra for (a) KCl and (b) KI, oriented with the ⟨001⟩ axis along the sample–detector line. The temperature is 35 K for KCl and 14 K for KI. The distinct narrow peaks at the centre and satellite peaks are observed at the projected momenta corresponding to $(G_x, G_y) = (2, 0)(2\pi/a)$ reciprocal-lattice vectors.

The KCl and KI samples were cleaved from high-purity single-crystal rods obtained from the University of Utah. The area of each sample facing the incident positrons was 2.0×7.0 mm^2. The sample was mounted on a cold finger of a closed-cycle helium refrigerator. The temperature was set at 15 ± 0.5 K for KI. It was set at 35 ± 0.5 K for KCl to diminish the effect of irradiation by positrons, which is noticeable below $\sim$30 K [14]. The reflection of a laser beam from a cleaved surface was used to orient the sample so

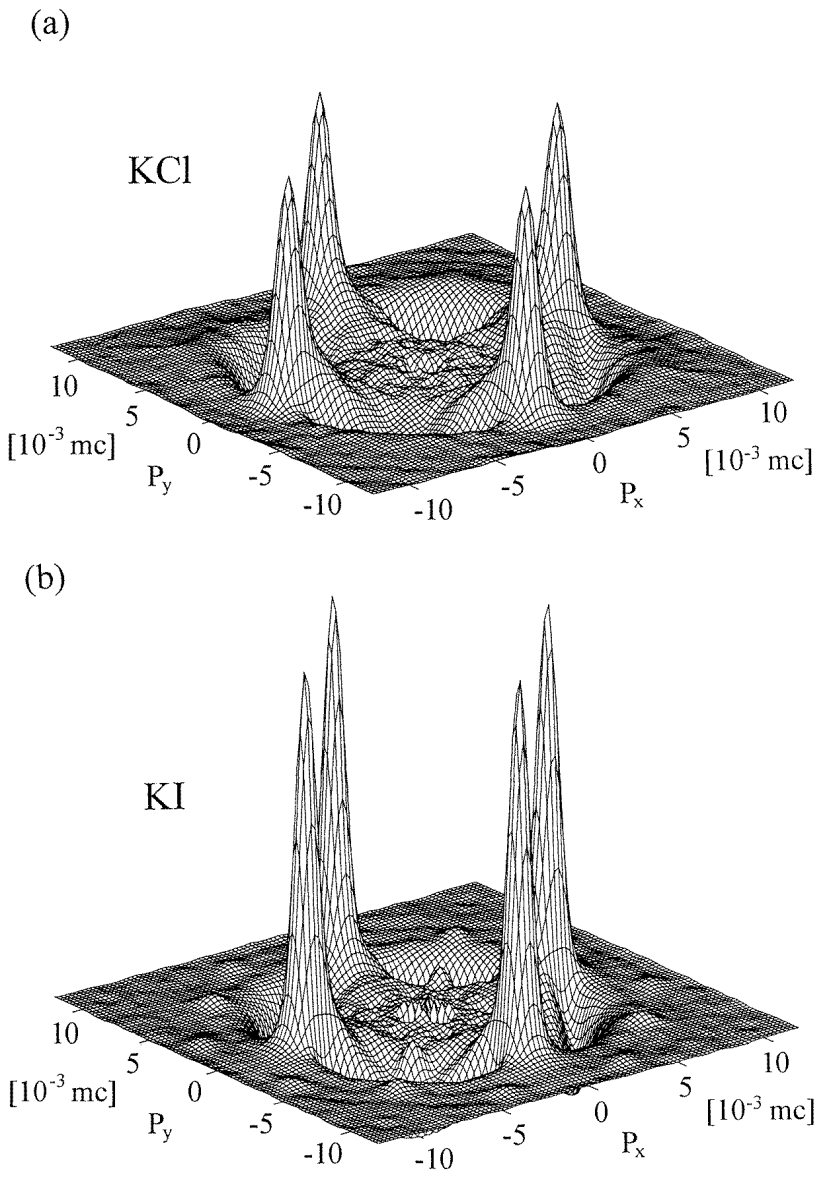

Figure 2. The anisotropy of the 2D-ACAR spectra shown in figure 1 for (a) KCl and (b) KI. Four kinds of peak, corresponding to $(2, 0)(2\pi/a)$, $(1, 1)(2\pi/a)$, $(2, 2)(2\pi/a)$, $(3, 1)(2\pi/a)$, are observed for KI, while no peaks except that corresponding to $(2, 0)(2\pi/a)$ are observed for KCl.

that the ⟨001⟩ axis of the crystal was parallel to the sample–detector line of the 2D-ACAR apparatus. This arrangement yields a projection of the electron–positron pair momentum distribution onto the (001) plane.

The distance between the sample and the positron source (∼30 mCi of ^{22}Na) placed outside a Be window of the sample chamber was about 10 mm. The positrons from the source were focused on the KI sample by a magnetic field of 1.25 T produced by an electromagnet. A lower magnetic field, 0.42 T, was applied to KCl, again to reduce the

irradiation effect.

3. Results

The 2D-ACAR spectrum obtained for KCl is shown in figure 1(a) and that for KI in figure 1(b), the total counts of which are 1.8×10^7 and 2.2×10^7, respectively. Distinct narrow peaks are seen at the momenta corresponding to the (001) projections $(G_x, G_y) = (0, 0)(2\pi/a)$ and $(2, 0)(2\pi/a)$ of the reciprocal-lattice vectors, where a is the fcc lattice constant. The intensity of a (G_x, G_y) projection peak represents the summation over G_z of the (G_x, G_y, G_z) components of the Ps momentum distribution:

$$\sum_{G_z} |u_G(0)|^2. \tag{6}$$

Figure 2 shows the anisotropies of the 2D-ACAR spectra obtained by subtracting the average of the distributions over $q = (p_x^2 + p_y^2)^{1/2}$. The peaks corresponding to the projections $(G_x, G_y) = (1, 1)(2\pi/a)$, $(2, 0)(2\pi/a)$, $(2, 2)(2\pi/a)$, and $(3, 1)(2\pi/a)$ are noticeable for KI. The $(2, 2)$ peaks, which overlapped with the $(2, 0)$ peaks in the previous 1D-ACAR data, are separately observed. The high sensitivity of the 2D measurement has permitted us to detect the (1, 1) peaks, which were not observed in the 1D measurements. For KCl, on the other hand, only the peaks corresponding to the $(G_x, G_y) = (2, 0)(2\pi/a)$ type of projections are noticeable even by anisotropy analysis of the present 2D-ACAR data. Figure 3 shows the angular cross-section of the anisotropy for $q = |(2, 0)|(2\pi/a)$ for KI. The intensity is normalized to that of the central peak. The relative intensities of the peaks were extracted from this and similar plots, and are listed in table 1.

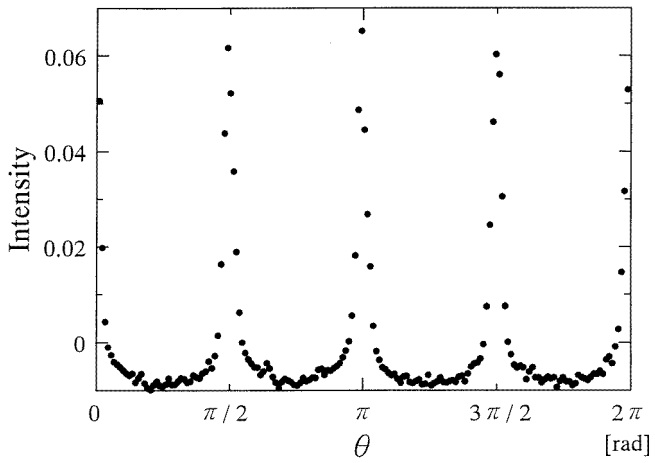

Figure 3. The distribution for $(p_x^2 + p_y^2)^{1/2} = |(2, 0)|(2\pi/a)$. The horizontal axis label (θ) means the angle between (p_x, p_y) and the p_x-axis.

4. Discussion

The 1D-projection sums of the peak intensities

$$\sum_{G_y, G_z} |u_G(0)|^2 \tag{7}$$

Table 1. The two-dimensional projection onto the (001) plane of the relative intensities of the central and satellite peaks for KCl and KI. The total intensity is normalized to 100%. The theoretical results calculated by orthogonalization and using the perturbation theory are also presented in the rows labelled 'Theory (I)' and 'Theory (II)', respectively. a_B is the Bohr radius.

			$(G_x, G_y)/(2\pi/a)$				
			(0, 0)	(1, 1)	(2, 0)	(2, 2)	(3, 1)
KCl	Experiment		$79 \pm 3\%$	$0 \pm 0.2\%$	$21 \pm 2\%$	$0 \pm 0.2\%$	$0 \pm 0.2\%$
	Theory (I)	$\lambda = 0.5a_B^{-1}$	91%	0.2%	7.6%	1.4%	0.1%
		$\lambda = 0.35a_B^{-1}$	84%	0.6%	13%	2.3%	0.2%
	Theory (II)		57%	5.0%	37%	1.4%	0%
KI	Experiment		$75 \pm 3\%$	$1.6 \pm 0.2\%$	$22 \pm 2\%$	$0.6 \pm 0.1\%$	$0.8 \pm 0.2\%$
	Theory (I)	$\lambda = 0.5a_B^{-1}$	92%	0.8%	5.7%	0.9%	0.4%
		$\lambda = 0.35a_B^{-1}$	87%	1.8%	8.8%	1.3%	0.7%
	Theory (II)		14%	57%	28%	1.3%	0%

Table 2. The one-dimensional projection onto the ⟨100⟩ axis of the relative intensities of the central and satellite Ps peaks for KCl and KI. The results calculated by Zhang and Song for KCl and those of the 1D-ACAR measurement by Kasai and Fujiwara for KI are shown in the rows labelled 'Theory (ZS)' and 'Experiment (KF)', respectively.

		$G_x/(2\pi/a)$			
		0	1	2	3
KCl	Experiment	$89 \pm 1\%$	0%	$11 \pm 1\%$	0%
	Theory (ZS)	81%	0%	19%	0%
KI	Experiment	$86 \pm 1\%$	$2.0 \pm 0.2\%$	$11 \pm 1\%$	$0.4 \pm 0.1\%$
	Experiment (KF)	88%	0%	12%	0%

are calculated from the present 2D data and listed in table 2. The corresponding values for KCl obtained by Zhang and Song [11] are also listed as 'Theory (ZS)'. The intensity of the $2(2\pi/a)$ peak is about 58% of the calculated result. The 1D-projection sums of the peak intensities for KI are compared with the corresponding results of the previous 1D-ACAR measurement by Kasai and Fujiwara [9]. The intensity of the $2(2\pi/a)$ peak for KI agrees with that of the previous 1D measurement; the intensities of the other satellite peaks were not detected in the 1D measurement.

The very low intensities of the odd-index peaks suggest that the Ps in alkali halides only vaguely distinguishes the anions from the cations regardless of the difference in the principal quantum numbers of the outermost closed shells of the ions. It is interesting that not only the odd-index peaks but also all of the satellite peaks except the $(2, 0)$ peaks are very weak in both crystals. This result is quite different from the case for quartz [1], in which the intensities of several different satellite peaks are relatively high.

We have explored whether these interesting features of the peak intensities can be explained by simple calculations. Two different approximations were tried. First we constructed the Ps wave function only by orthogonalizing its electron part to the electron wave functions for the ions [1]. In this approach the Coulomb interaction between the Ps

and the ions is neglected. The orthogonalized wave function is given by

$$\phi(\boldsymbol{r}_e, \boldsymbol{r}_p) = \phi_0(\boldsymbol{r}_e, \boldsymbol{r}_p) - \sum_i \varphi_i(\boldsymbol{r}_e) \int \phi_0(\boldsymbol{r}, \boldsymbol{r}_p)\varphi_i^*(\boldsymbol{r})\ \mathrm{d}^3\boldsymbol{r} \tag{8}$$

where $\phi_0(\boldsymbol{r}_e, \boldsymbol{r}_p)$ is taken to be the wave function of Ps in vacuum, $\exp(-\lambda|\boldsymbol{r}_e - \boldsymbol{r}_p|)$ ($\lambda = 0.5$ Bohr radii^{-1}), as the simplest approximation, and the $\varphi_i(\boldsymbol{r}_e)$ are the electron wave functions in the alkali halide. The electron wave functions in KCl or KI crystals evaluated by Kunz [15] were used. The calculated intensities of the Ps peaks are listed in table 1 as 'Theory (I)'. The very low intensities of the odd-index peaks are reproduced comparatively well for both crystals. However, the intensities of the $(2, 0)(2\pi/a)$ peaks are low (1/3–1/4) compared with those obtained from experiment. The ratio between the intensities of the satellite peaks $(2, 0)(2\pi/a)$ and $(2, 2)(2\pi/a)$ is not reproduced, either. Use of a smaller value of $\lambda = 0.35$ Bohr radii^{-1} resulted in an increase of the relative intensity of the satellite to central peaks, but the intensity of the $(2, 0)(2\pi/a)$ peaks was still too low.

In the second approximation [16], the exchange interaction of the electron in the Ps and the electrons in the crystal is neglected, and the Hamiltonian is approximated as

$$H = -\frac{\hbar^2}{2M}\Delta_{\boldsymbol{R}} - \frac{\hbar^2}{2\mu}\Delta_{\boldsymbol{r}} - \frac{e^2}{r} + eV\left(\boldsymbol{R} + \frac{\boldsymbol{r}}{2}\right) - eV\left(\boldsymbol{R} - \frac{\boldsymbol{r}}{2}\right) \tag{9}$$

where $\boldsymbol{R} = (\boldsymbol{r}_p + \boldsymbol{r}_e)/2$, $\boldsymbol{r} = \boldsymbol{r}_p - \boldsymbol{r}_e$, $M = 2m$, and $\mu = m/2$; $\pm eV$ are the potentials for the positron and the electron in Ps. The Ps wave function is constructed by treating the last two terms as perturbations. At least second-order perturbation is necessary if one is to discuss the intensities of the satellite peaks in this approximation, since the Coulomb interaction part in this approximation is an odd function of $\boldsymbol{r}$. The peak intensities calculated to second order are listed in table 1 as 'Theory (II)'. The intensities of the $(2, 0)(2\pi/a)$ peaks are higher than the experimental results, in contrast to the case for the orthogonalization calculation. The very low intensities of the odd-index peaks are not reproduced. The situation for KI appears to be outside the range of the perturbation theory.

From these calculations, it appears that the exchange interaction is essential for the very low intensities corresponding to the odd indices, while the Coulomb interaction is responsible for the high intensity of the $(2, 0)(2\pi/a)$ peak. The success of the calculations of Zhang and Song [11] in reproducing the vanishing odd-index peaks in KCl probably resulted from the inclusion of the exchange interaction in the Hamiltonian, and the use of the floating Gaussian orbital basis functions orthogonalized with respect to the electron states in the crystal. It should be noted, however, that the intensity of the $(2, 0)(2\pi/a)$ peak is not reproduced. Further studies are thus desirable.

In summary, the intensities of the Ps peaks in the 2D-ACAR spectra for KCl and KI were measured. Very low but finite intensities of the peaks with odd Miller index for KI were observed. Those for KCl were below experimental uncertainty. The intensities of the even-index peaks except that corresponding to (200) were also very low for both crystals. The intensity of the (200) peak for KCl was about half the theoretical value calculated by Zhang and Song. We tried to see to what extent two simple approximations for the wave functions of the delocalized Ps can explain the intensities of the peaks.

Acknowledgments

The authors wish to thank Professor Y Kubo, Professor O V Boev, and Dr I Bondarev for valuable discussions. This work was supported by a Grant-in-Aid for scientific research (No 08404018) from the Ministry of Education, Science and Culture of Japan. This work

was also supported in part by Research Fellowships of the Japan Society for the Promotion of Science for Young Scientists. The experiment was performed at the Radioisotope Centre of the University of Tokyo.

References

[1] Hodges C H, McKee B T A, Triftshauer W and Stewart A T 1972 *Can. J. Phys.* **50** 103
[2] Fujiwara K 1982 *Positron Annihilation* (Amsterdam: North-Holland) p 615
[3] Dupasquier M 1983 *Positron Solid State Physics* (Amsterdam: North-Holland) p 510
[4] Hyodo T 1985 *Positron Annihilation* (Singapore: World Scientific) p 643
[5] Brandt W, Coussot G and Paulin R 1969 *Phys. Rev. Lett.* **23** 522
[6] Mogensen O, Kvajic G, Eldrup M and Milosevic-Kvajic M 1971 *Phys. Rev.* B **4** 71
[7] Coussot G 1970 *PhD Thesis* University of Paris
[8] Kasai J, Hyodo T and Fujiwara K 1988 *J. Phys. Soc. Japan* **57** 329 and references therein
[9] Kasai J and Fujiwara K 1982 *J. Phys. Soc. Japan* **51** 3077
[10] Kittel C 1986 *Introduction to Solid State Physics* 6th edn (New York: Wiley) p 46
[11] Zhang C G and Song K S 1994 *J. Phys.: Condens. Matter* **6** 9173
[12] Zhang C G, Leung C H and Song K S 1994 *J. Phys.: Condens. Matter* **6** 7715
[13] Nagai Y, Saito H, Iwata T, Nagashima Y, Hyodo T, Uchida U and Omura T 1996 *Nucl. Instrum. Methods Phys. Res.* A **378** 629
[14] Kasai J, Hyodo T and Fujiwara K 1983 *J. Phys. Soc. Japan* **52** 3671
[15] Kunz A B 1971 *Phys. Rev.* B **4** 4164
[16] Boev O V and Arefiev K P 1984 *Phys. Status Solidi* b **125** 619